

# CONVECTIVE DISSOLUTION IN FIELD SCALE CO<sub>2</sub> STORAGE SIMULATIONS USING THE OPM FLOW SIMULATOR

Tor Harald Sandve<sup>1</sup>, Sarah E. Gasda<sup>1</sup>, Atgeirr Rasmussen<sup>2</sup>, Alf Birger Rustad<sup>3</sup>

<sup>1</sup> Norce, Bergen, Norway

<sup>2</sup> SINTEF, Oslo, Norway

<sup>3</sup> Equinor, Trondheim, Norway

\* Corresponding author e-mail: tor.harald.sandve@norce-research.no

## Abstract

In this work we introduce an accurate and efficient way of including the effect of convective mixing in field scale 3D simulations. The effect of the convective mixing is included in the field scale simulations by introducing a maximum dissolution rate given by the convective mixing. This maximum dissolution rate is computed internally based on both dynamic and static properties as well as a non-dimensional input parameter. The non-dimensional input parameter upscales the effect of the convective mixing and is estimated from fine-scale simulations. Our approach differs from existing models where the maximum dissolution rate is given directly as an input parameter to the simulator and not scaled by the properties of the cell. The proposed convective dissolution rate model shows good agreement with fine-scale simulation shown in this work as well as in the literature. The model is further tested on the 3D Sleipner Benchmark model. Results on the Sleipner Benchmark model confirm the importance of including the effect of the convective dissolution in the simulation both for the injection period and during the monitoring phase as it significantly affects the pressure build-up and decay during the simulations. The proposed model is implemented in the open source OPM Flow simulator which immediately makes it available to the community for usage and adoption. This paper also gives an overview of the CO<sub>2</sub> storage module implemented in OPM Flow.

**Keywords:** CO<sub>2</sub> storage simulations, Open-source software, The Sleipner Benchmark, CO<sub>2</sub> dissolution rate. Convective mixing.

## 1. Introduction

Numerical simulations form an important basis for decision-making processes for CO<sub>2</sub> storage. Good simulation models that incorporate the relevant physics on the relevant scale is thus important. Even with the continuing advances in available computational resources, simplification and upscaling of processes is necessary for practical simulation times. The dissolution of CO<sub>2</sub> into brine is one such important effect that needs to be considered. The main mechanism that drives the dissolution is convective mixing. Convective mixing happens on the centimeter scale and can therefore not be included in the model directly for field-scale model. It is suggested by several authors to include this effect as an upscaled dissolution rate [1][2][3][4].

Dissolution caused by convective mixing has been successfully implemented and demonstrated in research codes based on vertical equilibrium (VE) [4]. The approach involves incorporating an upscaled CO<sub>2</sub> mass transfer rate to account for sub-scale convection. CO<sub>2</sub> dissolves dynamically into the water column below, which is facilitated by the fact that a VE model is pseudo 2D and does not require vertical discretization.

VE models are a special class of 3D simulation where gravity segregation happens faster than simulated timescale and are especially useful in models of very large spatial and long timescales. However, many field-scale assessments of CO<sub>2</sub> storage still necessitate a 3D simulation to enable decision making. In this paper we adapt the suggested upscaled convective dissolution models to a 3D black oil setting and include it in the OPM Flow simulator.

The OPM Flow simulator [5] is an open-source community code that supports industry standard input and output format which allows for direct incorporation into existing simulation workflows. The base simulator is black oil, but it has many extensions that for instance allows for efficient modeling of CO<sub>2</sub>-EOR scenarios [6][7]. For details on the simulator, we refer to the technical paper [5] and the user manual [8].

The advantage of including the convective dissolution rate model in Flow is immediate access to industry standard I/O formats, and performance which allows for immediate testing on the Sleipner Benchmark model [9].

The CO<sub>2</sub> simulation in this work is done using the CO<sub>2</sub> storage module in OPM. This module builds on the CO<sub>2</sub>-brine fluid system in Dumux [10], but is adapted to

automatic differentiation (AD) as described in [5]. With AD the derivatives are automatically computed. This allows for simple extensions and modification of the code without losing neither accuracy in the Jacobian, nor significant performance, as shown in [11]. The AD framework thus allows for modification and implementation of new PVT models etc. in the code without significant effort and programming expertise.

## **2. CO<sub>2</sub> storage simulations in Flow**

Black oil simulators are commonly used in the industry to simulate CO<sub>2</sub> storage. They are attractive compared to more advanced compositional models due to availability, performance, and applicability into existing frameworks [12]. In black oil simulation the needed PVT properties are given as tabulated input values where brine properties correspond to oil and CO<sub>2</sub> to gas, using the standard black oil format. Tabulated input is very flexible but becomes cumbersome when for instance temperature effects or varying salinity etc. also needs to be considered.

A dedicated CO<sub>2</sub> storage module is therefore made available in the OPM Flow simulator. With the CO<sub>2</sub> storage option enabled Flow computes the PVT properties such as density, viscosity, and enthalpy internally as functions of pressure, temperature, and composition by using analytic correlations and models from the literature rather than by interpolation from tabulated values. These values are transformed to its black oil equivalents internally in the simulator. This thus gives us the accuracy of the compositional simulators while keeping the performance and applicability of the black oil simulator. The CO<sub>2</sub> storage module is enabled by adding the CO2STORE keyword to the input deck [8]. Note that a dedicated CO2STORE option is also available in the compositional Eclipse 300 simulator [13]. The internal models implemented in the CO2STORE option in OPM Flow are based on models found in the literature and does not correspond directly to the CO2STORE option implemented in Eclipse 300.

An overview of the implemented models in the 2021.04 version of Flow as used in this work now follows.

### **2.1 Brine-CO<sub>2</sub> PVT module.**

The density of water is given by the simplified formula presented in [14]. The formula gives significant speedup of the simulations without any significant loss of accuracy compared to using the formula in IAPWS 95 [15]. According to the authors in [14] average deviation is around 0.005% to IAPWS 95 for the relevant pressure and temperature range. Modification of the density due to dissolved CO<sub>2</sub> is accounted for using the correlation presented in [16], while salinity is accounted for using the correlation given in [17]. The density of the CO<sub>2</sub> is given by the Span-Wagner model [18]. The viscosity of brine is given using the correlation presented in [17], while the CO<sub>2</sub> viscosity is given by the correlation in [19]. The effect of the dissolved CO<sub>2</sub> on the liquid density is small and currently neglected.

CO<sub>2</sub> and brine are slightly miscible. CO<sub>2</sub> partitions into brine instantaneously until a solubility limit is reached locally (typically 2-5% by mass).

The solubility limit of CO<sub>2</sub> and brine depends on temperature, pressure and salinity and is implemented according to [20], where the activity coefficients of CO<sub>2</sub> in brine are taken from [21]. The solubility limit gives an upper bound of the amount of CO<sub>2</sub> that can dissolve into the brine.

### **2.2 Thermal properties**

No simulations with thermal effects are shown in this paper, but for completeness the thermal properties used in the CO<sub>2</sub> storage module is presented here. For thermal simulations, the enthalpy of the fluids needs to be computed. The CO<sub>2</sub> enthalpy is computed according to [18] and is represented as a table internally in the simulator. The liquid enthalpy depends on the dissolved CO<sub>2</sub> and salinity as well as pressure and temperature. The water enthalpy is given according to IAPWS 97 [22] and modified to account for salinity according to [23] and for CO<sub>2</sub> following [21].

Thermal conductivity and rock heat capacity is input parameters to the simulator and must be provided by the user. See the OPM manual for details on usage of the thermal simulator [8].

### **2.4 Diffusion**

For field-scale simulations diffusion is a sub-grid phenomenon and is typically not explicitly represented in the equations. For simulations on the laboratory scale diffusion plays a direct role and therefore needs to be explicitly represented in the equations. The diffusion coefficients that control the diffusion depends on temperature, pressure, and salinity. The diffusion coefficient is computed internally for pure water using [24] and modified to account for salinity using [25]. The effect of the porous media on the diffusion is modeled using the relation suggested in [26]. The coefficient can also be given as an input parameter using the DIFFC keyword. The effect of diffusion is included in the fine-scale simulation in section 4.1.

## **3. Controlling the dissolution rate.**

For field scale simulations a typical grid block size is tens or even hundreds of meters in the horizontal direction and typically a few meters in the vertical direction. The density difference between CO<sub>2</sub> in gas (or super critical) phase and brine leads to rapid phase segregation. The lighter CO<sub>2</sub> moves quickly to the top of the reservoir or to an intermediate sealing layer and then migrates along the sealing layer. For cells where a vertical equilibrium is reached only the top layer of the cell is exposed to the free CO<sub>2</sub> and a fully mixture of the CO<sub>2</sub> and brine cannot be assumed. A direct use of the solubility models presented in section 2.1 will thus over-estimate the amount of dissolved CO<sub>2</sub> in brine in these cells if used directly.

The dissolution process in these cells is controlled by the convective mixing. Since brine with dissolved CO<sub>2</sub> is slightly heavier than without, instabilities will occur at the phase boundary in form of heavier fingers of brine with dissolved CO<sub>2</sub> migrating downwards. These fingers happen on the centimeter scale and can therefore not be included directly in field-scale simulations. Instead, the effect of convective mixing is included through a control of the dissolution rate. The convective mixing depends on both dynamic and static properties of the reservoir but dimensional analyses in [2] suggested a scaling for the dissolution rate that allows for usage of a single parameter. The dissolution rate  $F$  in kg / (m<sup>2</sup>s) in [2] is given as

$$F = \chi c_{max} K_z \Delta \rho_c g / \mu \quad (1)$$

where  $\chi$  is a non-dimensional parameter controlling the dissolution,  $c_{max}$  is the maximum concentration at the solubility limit,  $K_z$  is the vertical permeability and  $\Delta \rho_c$  is the difference of the brine density at maximum amount of dissolved CO<sub>2</sub> and the density without dissolved CO<sub>2</sub>. Finally,  $g$  is the gravity constant,  $\mu$  the viscosity.

To use equation (1) in the OPM Flow simulator we first need to convert it to a black oil setting. In the black oil model, the amount of dissolved gas in the liquid (i.e., oil) phase is given by the solution gas/oil ratio (RS). The standard metric unit of RS is SM<sub>3</sub>/SM<sub>3</sub>. The solution gas/oil ratio or gas dissolution factor is related to the mass fraction as following.

$$RS \stackrel{\text{def}}{=} \frac{V_{g,ref}}{V_{o,ref}} = \frac{x_o^g \rho_{o,ref}}{1 - x_o^g \rho_{g,ref}} \quad (2)$$

Here  $x_o^g$  is the mass fraction of gas in the oil phase and  $\rho_{o,ref}$ ,  $V_{o,ref}$  and  $\rho_{g,ref}$ ,  $V_{g,ref}$  are the density and volume of the oil and gas at reference conditions, respectively.

In the black oil model, the dissolution rate (DRSDT) is defined as the maximum rate at which the solution gas-oil ratio (RS) can be increased in a grid cell per time.

To convert equation (1) into a black oil formulation we first need to replace the maximum concentration at the solubility limit used in the equation (1) with its black oil equivalent,  $RS_{SAT}$ .

$$\begin{aligned} RS_{SAT} &\stackrel{\text{def}}{=} \frac{V_{CO_2,max,ref}}{V_{brine,ref}} \\ &= \frac{m_{CO_2,max}}{V_{brine} B_{brine} \rho_{CO_2,ref}} \\ &= \frac{c_{max}}{B_{brine} \rho_{CO_2,ref}} \end{aligned} \quad (3)$$

Here  $m_{CO_2,max}$  is the mass of CO<sub>2</sub> at the maximum solubility limit and  $B_{brine}$  the formation volume factor of brine.

The next step is to convert  $F$  in (1) from kg/(m<sup>2</sup>s) to change in RS (gas-oil volume ratio under reference conditions) per day. We do this by multiplying with the cell top face area ( $A$ ) and a conversion factor  $\tau = 86400 \text{ s/day}$ , then dividing by the volume of the brine and the density of the CO<sub>2</sub> both at reference condition.

$$\frac{\tau FA}{V_{brine,ref} \rho_{CO_2,ref}} = \frac{\tau FA}{V S_{brine} \phi \rho_{CO_2,ref} B_{brine}} \quad (4)$$

where  $V$  is the cell volume,  $S_{brine}$  is the brine saturation,  $\phi$  the porosity. We further assume  $V \approx AD_z$  to replace  $A/V$  with the cell thickness  $D_z$ . Combining equation (3) and (4) gives the following expression for the maximum dissolution rate DRSDT (SM<sub>3</sub>/(SM<sub>3</sub> day))

$$DRSDT = \chi \tau \frac{RS_{sat} K_z \Delta \rho_c g}{\mu S_{brine} D_z \phi} \quad (5)$$

According to analysis in [2], 0.04 is a reasonable value for  $\chi$  for the Utsira formation. Improved estimates on  $\chi$  can be computed using either numerical fine-scale simulations (see Section 4.1) or based on laboratory tests [3]. The simulation results are sensitive to the choice of  $\chi$  and some range of uncertainty in the parameter is thus recommended. The  $\chi$  value can further be constrained using gravimetric and/or seismic data from the field [27].

In commercial simulators like Eclipse a constant or regional value for DRSDT can be given as an input parameter. The DRSDT can be used to include the effect of convective mixing as shown for instance in [28]. Our approach differs from this in that the DRSDT value is computed internally and now depends on both static and dynamic cell properties.

To use the convective dissolution rate control given in equation in (5) in the Flow simulator a keyword DRSDTCON needs to be given with the non-dimensional  $\chi$  parameter. See the OPM Flow manual for more details [8].

Note that the convective dissolution rate assumes that the cell is in vertical equilibrium an assumption that is not always fulfilled in near well regions and in heterogenous reservoirs with low vertical permeabilities. A purely convective dissolution rate thus under-estimates the dissolution in the area around the injection well where CO<sub>2</sub> migrates upwards due to buoyancy. We expect a hybrid approach where the dissolution is not restricted by the convective dissolution in the upcoming regions to remedy this. Efforts to define robust and accurate criteria for detecting these cells are ongoing.

## 4. Simulation results

In this section we present simulation results that demonstrate usage of the convective dissolution rate control in OPM Flow. All simulations are done using the CO<sub>2</sub> storage option (CO2STORE).

### 4.1 Fine-scale simulations

We start with fine-scale simulations that illustrates the dissolution process and gives estimates on the non-dimensional  $\chi$  parameter given in equation (5). For this we use a column with 5-meter width and 10-meter height. Initially the column is filled with a 2-meter layer of free CO<sub>2</sub> on the top. A free boundary is set on the bottom to avoid pressure build-up. We discretize the domain using cells of size 0.01 m x 0.01 m. The computed dissolution rate is sensitive to the grid resolution, but we believe the given grid resolution is sufficient for the illustrative purpose of this example. Note that the given grid

resolution results in a simulation model with half a million cells.

The parameters and setup are based on the Sleipner benchmark and are given in Table 1. The capillary transmission zone plays an important role in enhancing the dissolution process [2]. In this study we compute the relative permeability and capillary pressure using the Brooks Corey model. An entry pressure of 2.5kPa and a Brooks Corey parameter of 2.8 is used as suggested in [29].

Note that diffusion plays an important role in triggering the convective mixing and is therefore included in these simulations. The diffusion coefficient for CO<sub>2</sub> in brine for the pressure, temperature, and salinity in using the models given in Section 2.4 is 3.0e-9 m<sup>2</sup>/s. Also, a small perturbation of the porosity ( $\pm 0.04$ ) is added to create sufficient instabilities in the model. The dissolution rate is not sensitive to these perturbations.

A snapshot of the dissolved CO<sub>2</sub> in brine (RS) is shown in Figure 1 after 60 days of simulation. The figure shows the classical fingering phenomena caused by the convective mixing. Note that we stop the simulation after 60 days to avoid boundary effects due to arrival of dissolved CO<sub>2</sub> to the bottom of the domain.

Figure 2 shows the dissolution of CO<sub>2</sub> in brine through the simulation. Apart from some initial dissolution caused by the capillary transmission zone we observe how the dissolution increases linearly with time. The linear coefficient gives us the convective dissolution rate. From linear regression we estimate the linear coefficient  $DRS_{DT} = 0.0064$  (SM<sup>3</sup>/(SM<sup>3</sup> day)). With this value for  $DRS_{DT}$  and the average dynamic properties given in Table 1, Equation (5) gives us  $\chi = 0.034$ . This is in line with the value 0.04 reported in [2]. Inserting  $\chi = 0.034$  in Equation (1) gives  $F = 12.5$  kg / (m<sup>2</sup> year) which again aligns with the numerical sensitivity study reported in [1].

Improving the grid resolution and/or doing fine-scale 3D simulations could give better estimates of the  $\chi$  parameter, but some uncertainty always remains due to impact of local heterogeneities etc. in the physical world.

Table 1: Input properties used for the fine-scale simulation and in the evaluation of equation (4) in Section 4.1.

Property	Value
Porosity	0.36
Permeability	2000 mD
Rock compressibility	1e-6 barsa <sup>-1</sup>
Salinity	0.7 gm-M/kg
Pressure	200 barsa
Temperature	50 °C
$RS_{sat}$	27.04 SM <sup>3</sup> /SM <sup>3</sup>
$\Delta\rho_c$	10 kg/m <sup>3</sup>
$S_{brine}$	0.8
$D_z$	10 m
$\mu$	0,85 cP

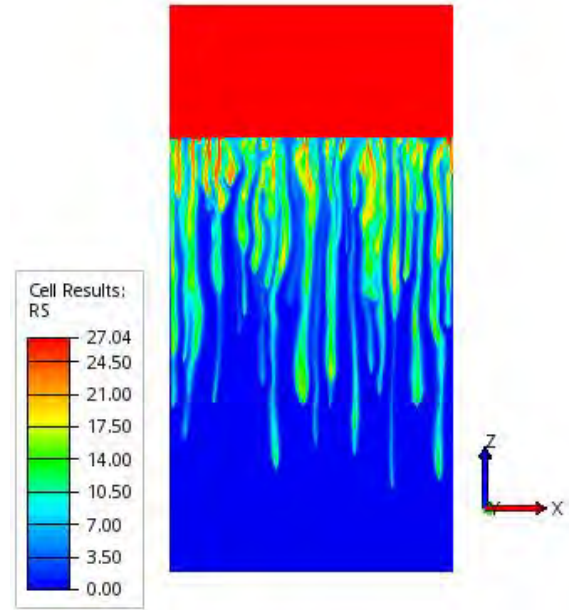


Figure 1: Dissolved CO<sub>2</sub> after 60 days of simulation for the fine-scale case.

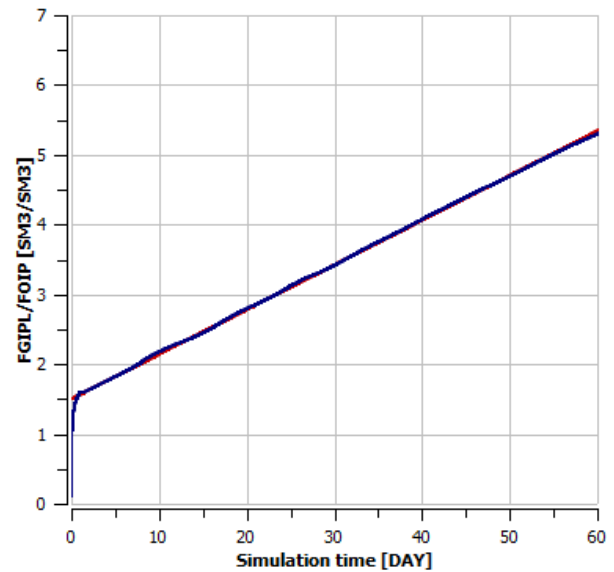


Figure 2: Estimated CO<sub>2</sub> dissolution (FGIPL/FOIP) from fine-scale simulations (blue) and linear function  $RS = 0,0064 * \text{day} + 1.5$  (red). The 0,0064 is the convective dissolution rate while the 1.5 constant comes from the capillary transition zone.

#### 4.2 Sleipner simulation results

The Sleipner benchmark model [9] recently released by Equinor will be the base model for demonstrating our approach. For simplicity, the mean values presented in the dataset are used for the porosity and the permeability of the layers, while all feeders are assumed to have permeability 2000mD. We use the same relative permeability and capillary pressure and salinity as in the fine-scale simulations. Initially we assume hydrostatic

pressure with 146 bar at 863 meters depth. A constant temperature gradient is imposed throughout the simulation defined by 30 C at 800 meters depths and 41 C at 1000 meters depths.

We further assume CO<sub>2</sub> is injecting at a constant injection rate of 1.46 million SM<sup>3</sup> / day (1.0Mt / year) from 1st of September 1996 and until the end of 2010. After the injection is stopped the simulations continue for 200 years.

To investigate the effect of the upscaled convective mixing we use  $\chi = 0.034$  and compare it with a base case without dissolution of CO<sub>2</sub>. Figure 3 compares the total amount of CO<sub>2</sub> with the amount that is dissolved during the simulation period. During the injection period this shows that approximately 0.5% of the CO<sub>2</sub> dissolves into the brine pr year which is one third of the upper bound of 1.8% pr year estimated using gravity monitoring in [27]. As discussed in Section 3, a purely convective dissolution rate under-estimates the dissolution in the area around the injection well where CO<sub>2</sub> migrates upwards due to buoyancy and a lower value for the injection period is thus expected.

According to these simulations almost 60% of the CO<sub>2</sub> is dissolved into the brine 200 years after the injection period. Using the definition in (2) a global average RS can be computed by dividing the amount of dissolved CO<sub>2</sub> to the amount of oil in place which is approximately 2.0e9 SM<sup>3</sup>. This gives an average RS value of 2.2 which is still significantly lower than the theoretical limit given by  $RS_{sat}$  which is approximately 30 for the range of pressure, temperature, and salinity relevant for the Sleipner case. In other words, a significant part of the reservoir is still not reached by the injected CO<sub>2</sub>. Figure 4 shows the development of the average reservoir pressure during the simulation period. For the case without dissolution of CO<sub>2</sub> the pressure reaches its maximum value (330 bar) when the injection stops and stays constant during the next 200 years. This is as expected since the model assumes closed boundaries. For the case with convective dissolution rate the pressure reaches its maximum at the same time, but the maximum value (316 bar) is 14 bar less than for the case without dissolved CO<sub>2</sub>. The pressure then gradually decreases as more CO<sub>2</sub> dissolves into the brine. This is again expected since the density of brine increases as CO<sub>2</sub> dissolves into it. Note that the results are sensitive to the choice of  $\chi$ , and the uncertainty of  $\chi$  therefore should be incorporated into the simulations by for instance using an ensemble of simulations to gain confidence in the results. We also believe the dissolution rate and in particular  $\chi$  to be an important history matching parameter as also claimed in for instance [27].

Snapshots of the amount of dissolved CO<sub>2</sub> and the CO<sub>2</sub> saturation are shown in Figure 5 and Figure 6, respectively. The snapshots are taken at the J-K plane going through the well at the end of the injection period and at the end of the simulations for the case with the convective dissolution rate. In all the figures we clearly see the characteristic layered structure of the Sleipner model. The CO<sub>2</sub> rapidly migrated to the top through the “chimneys” that acts as holes in the shale layers. What is

noticeable in Figure 5 is that most of the free CO<sub>2</sub> has disappeared after the 200-year period without injection. The remaining free CO<sub>2</sub> is gathered in a few structural traps. The top snapshot in Figure 6 shows that the dissolution process is significant also during the injection period as CO<sub>2</sub> slowly dissolves and migrating downwards given the characteristic fingering phenomena. After 200 years we observe how the “chimneys”, where the free CO<sub>2</sub> used to move upwards during the injection, now acts as sinks for the CO<sub>2</sub> rich brine. A significant portion of the stored CO<sub>2</sub> is thus securely stored in the bottom layer.

The released Sleipner model has approximately 2 million cells. For practical simulation times we have therefore used our internal cluster that allows for usage of 64 CPUs with two threads each. We observe a near ideal scaling of the simulation time for the tested range of CPUs for this model.

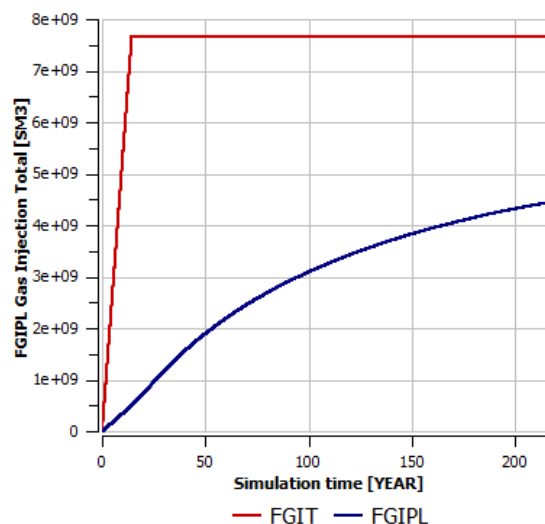


Figure 3: The amount of dissolved CO<sub>2</sub> in the liquid phase (FGIPL) compared to the total amount of injected gas (FGIT) for the case with the convective dissolution rate.

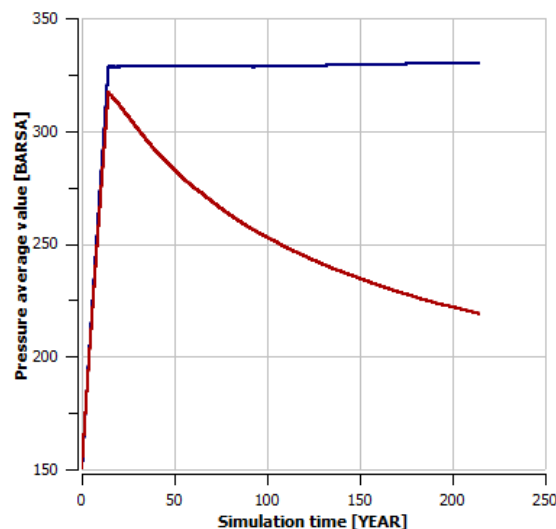


Figure 4: Field average pressure for the case without (blue) and with (red) dissolution of CO<sub>2</sub>.

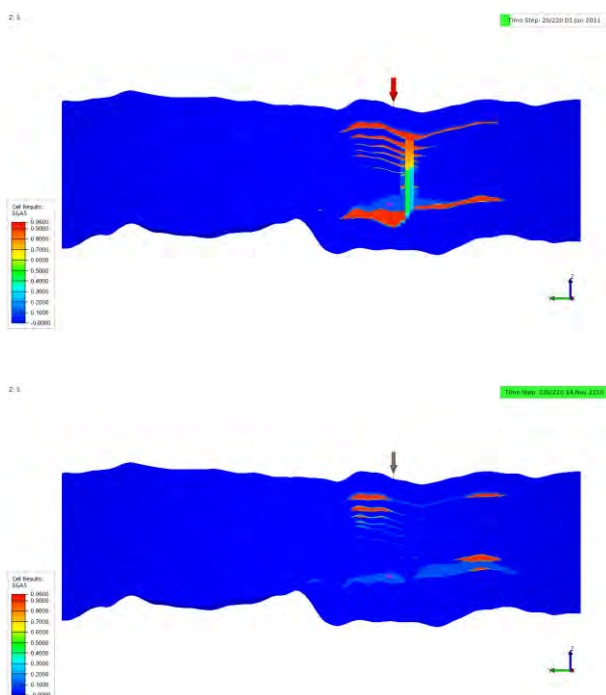


Figure 5: CO<sub>2</sub> saturation after the injection period (top) and after 200 years of storage (bottom).

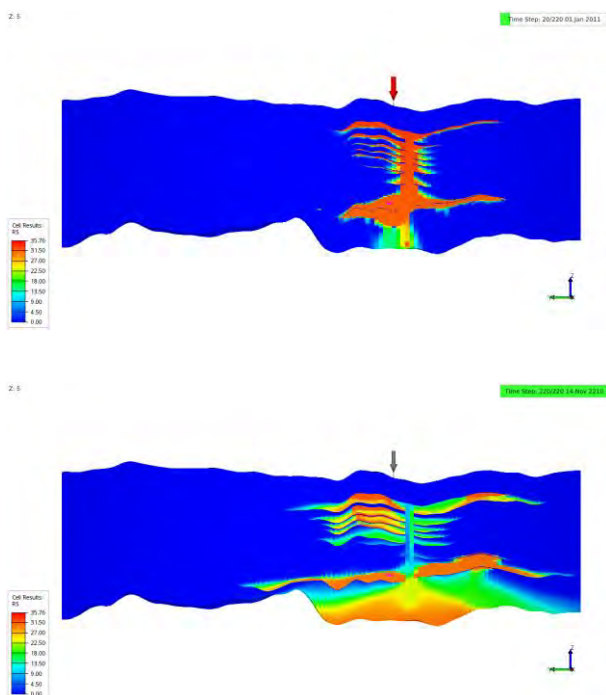


Figure 6: Dissolved CO<sub>2</sub> after the injection period (top) and after 200 years of storage (bottom).

## 5. Summary

A model for upscaling the effect of convective mixing through a convective dissolution rate control is implemented in the open-source simulator OPM Flow. The upscaled approach allows for efficient and accurate inclusion of the impact of convective mixing in field scale 3D simulations. The simulation results on the Sleipner Benchmark model agree well with the impact of

convective dissolution reported in the literature. Ongoing work on defining robust and accurate criteria for detecting cells where the convective dissolution rate is the dominant dissolution factor will further improve the accuracy and applicability of our approach.

All simulations in our work are done using the CO<sub>2</sub> storage module in OPM Flow. This dedicated CO<sub>2</sub> storage module simplifies usage of the simulator for CO<sub>2</sub> storage applications while maintaining the needed accuracy in the fluid properties of the CO<sub>2</sub>-brine system. The implementation of the dissolution rate control in the OPM Flow simulator further gives immediate access to state-of-the-art parallel simulation capabilities and industry standard I/O which allows for immediate testing and usage on relevant field scale models.

## Acknowledgements

The authors would like to acknowledge financial support from the CLIMIT-Demo/Gassnova project 620073.

## References

- [1] Mykkeltvedt, T. S., & Nordbotten, J. M. (2012). Estimating effective rates of convective mixing from commercial-scale injection. *Environmental Earth Sciences*, 67(2), 527-535.
- [2] Elenius, M. T., Nordbotten, J. M., & Kalisch, H. (2014). Convective mixing influenced by the capillary transition zone. *Computational Geosciences*, 18(3-4), 417-431.
- [3] Taheri, A., Torsæter, O., Lindeberg, E., Hadia, N. J., & Wessel-Berg, D. (2018). Qualitative and quantitative experimental study of convective mixing process during storage of CO<sub>2</sub> in heterogeneous saline aquifers. *International Journal of Greenhouse Gas Control*, 71, 212-226.
- [4] Gasda, S. E., Nordbotten, J. M., & Celia, M. A. (2012). Application of simplified models to CO<sub>2</sub> migration and immobilization in large-scale geological systems. *International Journal of Greenhouse Gas Control*, 9, 72-84.
- [5] Rasmussen, A. F., Sandve, T. H., Bao, K., Lauser, A., Hove, J., Skaflestad, B., ... & Thune, A. (2021). The open porous media flow reservoir simulator. *Computers & Mathematics with Applications*, 81, 159-185.
- [6] Sandve, T. H., Rasmussen, A., & Rustad, A. B. (2018, October). Open reservoir simulator for CO<sub>2</sub> storage and CO<sub>2</sub>-EOR. In *14th Greenhouse Gas Control Technologies Conference Melbourne* (pp. 21-26).
- [7] Sandve, T. H., & Aavatsmark, I. (2020, September). Improved Extended Blackoil Formulation for CO<sub>2</sub>EOR Simulations. In *ECMOR XVII (Vol. 2020, No. 1, pp. 1-22)*. European Association of Geoscientists & Engineers.
- [8] The Open Porous Media Team. OPM Flow Reference Manual 2020-10. <https://opm-project.org/>
- [9] Equinor. Sleipner 2019 Benchmark Model <https://CO2datashare.org/dataset/sleipner-2019-benchmark-model> DOI:10.11582/2020.00004
- [10] Flemisch, B., Darcis, M., Erbertseder, K., Faigle, B., Lauser, A., Mosthaf, K., ... & Helmig, R. (2011). DuMux: DUNE for multi-{phase, component, scale, physics,...} flow and transport in porous media. *Advances in Water Resources*, 34(9), 1102-1112.

- [11] Lauser, A., Rasmussen, A. F., Sandve, T. H., & Nilsen, H. M. (2018, September). Local forward-mode automatic differentiation for high performance parallel pilot-level reservoir simulation. In ECMOR XVI-16th European Conference on the Mathematics of Oil Recovery (Vol. 2018, No. 1, pp. 1-12). European Association of Geoscientists & Engineers.
- [12] Hassanzadeh, H., Pooladi-Darvish, M., Elsharkawy, A. M., Keith, D. W., & Leonenko, Y. (2008). Predicting PVT data for CO<sub>2</sub>-brine mixtures for black-oil simulation of CO<sub>2</sub> geological storage. *international journal of greenhouse gas control*, 2(1), 65-77.
- [13] Schlumberger, ECLIPSE Industry-Reference Reservoir Simulator – Technical Manual 2016.1.
- [14] Hu, J., Duan, Z., Zhu, C., & Chou, I. M. (2007). PVTx properties of the CO<sub>2</sub>-H<sub>2</sub>O and CO<sub>2</sub>-H<sub>2</sub>O-NaCl systems below 647 K: Assessment of experimental data and thermodynamic models. *Chemical Geology*, 238(3-4), 249-267.
- [15] Wagner, W., & Pruß, A. (2002). The IAPWS formulation 1995 for the thermodynamic properties of ordinary water substance for general and scientific use. *Journal of physical and chemical reference data*, 31(2), 387-535.
- [16] Garcia, J. E. (2001). Density of aqueous solutions of CO<sub>2</sub> (No. LBNL-49023). Lawrence Berkeley National Lab. (LBNL), Berkeley, CA (United States).
- [17] Batzle, M., & Wang, Z. (1992). Seismic properties of pore fluids. *Geophysics*, 57(11), 1396-1408.
- [18] Span, R., & Wagner, W. (1996). A new equation of state for carbon dioxide covering the fluid region from the triple-point temperature to 1100 K at pressures up to 800 MPa. *Journal of physical and chemical reference data*, 25(6), 1509-1596.
- [19] Feghhour, A., Wakeham, W. A., & Vesovic, V. (1998). The viscosity of carbon dioxide. *Journal of physical and chemical reference data*, 27(1), 31-44.
- [20] Spycher, N., Pruess, K., & Ennis-King, J. (2003). CO<sub>2</sub>-H<sub>2</sub>O mixtures in the geological sequestration of CO<sub>2</sub>. I. Assessment and calculation of mutual solubilities from 12 to 100 C and up to 600 bar. *Geochimica et cosmochimica acta*, 67(16), 3015-3031.
- [21] Duan, Z., & Sun, R. (2003). An improved model calculating CO<sub>2</sub> solubility in pure water and aqueous NaCl solutions from 273 to 533 K and from 0 to 2000 bar. *Chemical geology*, 193(3-4), 257-271.
- [22] Wagner, W., & Kruse, A. (2013). Properties of Water and Steam/Zustandsgrößen von Wasser und Wasserdampf: The Industrial Standard IAPWS-IF97 for the Thermodynamic Properties and Supplementary Equations for Other Properties/Der Industrie-Standard IAPWS-IF97 für die thermodynamischen Zustandsgrößen und ergänzende Gleichungen für andere Eigenschaften. Springer-Verlag.
- [23] Daubert, T. E., Daubert, T. E., & Danner, R. P. (1989). Physical and thermodynamic properties of pure chemicals: Data compilation. Washington, DC: Taylor & Francis.
- [24] McLachlan, C. N. S., & Danckwerts, P. V. (1972). Desorption of carbon dioxide from aqueous potash solutions with and without the addition of arsenite as a catalyst. *Trans. Inst. Chem. Eng*, 50, 300-309.
- [25] Ratcliff, G. A., & Holdcroft, J. G. (1963). Diffusivities of gases in aqueous electrolyte solutions. *Trans. Inst. Chem. Eng*, 41(10), 315-319.
- [26] Millington, R. J., & Quirk, J. P. (1961). Permeability of porous solids. *Transactions of the Faraday Society*, 57, 1200-1207.
- [27] Alnes, H., Eiken, O., Nooner, S., Sasagawa, G., Stenvold, T., & Zumberge, M. (2011). Results from Sleipner gravity monitoring: Updated density and temperature distribution of the CO<sub>2</sub> plume. *Energy Procedia*, 4, 5504-5511.
- [28] Thibeau, S., & Dutin, A. (2011). Large scale CO<sub>2</sub> storage in unstructured aquifers: Modeling study of the ultimate CO<sub>2</sub> migration distance. *Energy Procedia*, 4, 4230-4237.
- [29] Cavanagh, A. (2013). Benchmark calibration and prediction of the Sleipner CO<sub>2</sub> plume from 2006 to 2012. *Energy Procedia*, 37, 3529-3545.